# Ultrahigh-sensitivity label-free optical fiber biosensor based on a tapered singlemode- no core-singlemode coupler for *Staphylococcus aureus* detection

**Ling Chen[a,b,#], Yuan-Kui Leng[c,#], Bin Liu[a,*], Juan Liu[a], Sheng-Peng Wan[a], Tao Wu[a], Jinhui Yuan[d,*], Liyang Shao[e], Guoqiang Gu[e], Yong Qing Fu[b], Hengyi Xu[c], Yonghua Xiong[c], Xing-Dao He[a] and Qiang Wu[a, b, *]**

[a]*Key Laboratory of Nondestructive Test (Ministry of Education), Nanchang Hangkong University, Nanchang 330063, China*

[b]*Faculty of Engineering and Environment, Northumbria University, Newcastle Upon Tyne, NE1 8ST, United Kingdom*

[c]*State Key Lab Food Sci & Technol, Nanchang University, Nanchang, Peoples R China*

[d]*Research Center for Convergence Networks and Ubiquitous Services, University of Science & Technology Beijing, Beijing 100083, China*

[e]*Department of Electrical and Electronic Engineering, Southern University of Science and Technology of China, Shenzhen, Peoples R China*

*# These authors have equal contributions to this paper*

** Corresponding authors: qiang.wu@northumbria.ac.uk; liubin_d@126.com; yuanjinhui81@163.com*

**Abstract**

An ultra-high sensitivity label-free optical fiber biosensor for inactivated *Staphylococcus aureus* (*S. aureus*) detection is proposed and investigated in this study, with additional advantages of robust and stability compared to traditional tapered fiber structure. The proposed fiber biosensor is based on a tapered singlemode- no core-singlemode fiber coupler (SNSFC) structure, where the no core fiber was tapered to small diameter (taper-waist diameter of about 10 μm) and functionalized with the pig immunoglobulin G (IgG) antibody for detection of *S. aureus*. The measured maximum wavelength shift of the sensor for an *S. aureus* concentration of $7\times10^1$ CFU/ml (colony forming unit per milliliter) is 2.04 nm, which is equivalent to a limit of detection (LOD) of 3.1 CFU/ml (a highest LOD reported so far for optical fiber biosensors), considering the maximum wavelength variation of the sensor in phosphate buffered saline (PBS) is ±0.03 nm over 40 minutes, where 3 times of maximum wavelength variation (3×0.03=0.09 nm) is defined as measurement limit. The response time of the developed fiber sensor is less than 30 minutes. The ultra-sensitive biosensor has potential to be widely applied to various areas such as disease, medical diagnostics and food safety inspection.

**Keywords:** Optical fiber sensor, biosensor, *Staphylococcus aureus* (*S. aureus*), foodborne pathogens.

## 1. Introduction

*Staphylococcus aureus* (*S. aureus*), firstly discovered by Dr. Alexander Ogston in 1880, is a type of spherical bacteria with a diameter of about 0.8 μm and arranged like a cluster of grapes under the microscope without spores [1]. *S. aureus* is one of the most common foodborne pathogens and often parasitic on human and animal skin, nasal cavity, stomach, air and sewage, which can produce variety of toxins causing diseases, such as pneumonia, pus infections and pericarditis, etc [2-5]. In order to avoid the diseases caused by *S. aureus*, it is crucial to achieve rapid and highly sensitive detection of *S. aureus* before the contaminated food is consumed. The traditional detection methods for the detection of *S. aureus* are culture-based assay, which normally requires several days to culture the bacteria before the results can be obtained. Most foods are contaminated with fewer pathogen cells [normally less than 100 CFU/g (Colony Forming Unit per gram)]. Therefore, an initial enrichment of the sample is needed with the traditional methods. However, the products are minimally processed and have an inherently short shelf life, which limited the application of these traditional methods. Hence, there is an urgent need to develop a high sensitivity, rapid detection method for foodborne pathogens. In recent years, some rapid detection technologies have been developed, such as polymerase chain reaction (PCR) [6-7], enzyme linked immunosorbent assay (ELISA) [8] and nucleic acid-based molecular biology methods [9]. For example, Majumdar *et al* reported an electrochemical biosensor for detection of *S. aureus* by depositing antibody on the surface modified platinum electrode, which achieved a limit of detection (LOD) of 10 CFU/ml. However, these electrochemical biosensors have disadvantages of generating false current values due to the

existence of different electro-active compounds, thus often leading to interferences and hence measurement errors [10]. In 2017, Menti *et al* developed a mass-based biosensor based on the magneto-elastic method for *S. aureu*s detection. However, this technique has been limited with a relatively poor LOD of $10^4$ CFU/ml and complicated operation processes [11-12].

In comparison with these techniques, optical biosensors have unique advantages such as high sensitivity, simple fabrication processes, capability for real time monitoring and robust to environments, which are widely investigated for detection of pathogens [13]. Depending on different working principles, optical biosensors can be divided into different categories, including fiber grating [14-15], surface plasmon resonance (SPR) [16], tapered optical fiber [17-18], surface enhanced Raman spectroscopy (SERS) [19], colorimetric sensor [20], fluorescence [21], U-bent fiber [22] and optical fiber interferometry [23]. For example, Tripathi *et al* adopted a long period grating modified with T4 bacteriophage to detect *Escherichia coli* (*E.coli*) and achieved an LOD of $10^3$ CFU/ml [24]. A tapered fiber biosensor was developed to specifically identify dead *E. coli O157:H7* and obtained an LOD of $10^4$ CFU/ml [25]. Janczuk-Richter *et al* demonstrated a long period grating based biosensor for T7 bacteriophage detection and achieved an LOD less than $5\times10^3$ CFU/ml [26]. Abdelhamid and Wu *et al* utilized fluorescence optical biosensors to detect *S. aureus* and achieved an LOD of $2 \times 10^2$ CFU/ml [27]. Most recently, Kumar *et al* developed an ultra-highly sensitive biosensor based on tapered no-core fiber structure for human chorionic gonadotropin (hCG) detection with an LOD of 0.0001 mIU/ml [28]. The tapered fiber interferometer provides an ultrahigh sensitivity, however due to a very small diameter (~10 μm) of the taper waist, this type of sensor is fragile with relatively poor stability. In this paper, we propose a novel tapered fiber biosensor based on tapered no-core fiber coupler structure, which has a much larger taper waist diameter (double waist diameter of a single taper fiber and hence robust with a better stability) without sacrificing the sensitivity, and applied it for detection of *S. aureus*.

## 2. Sensor structure

Figure1 shows a schematic diagram of the tapered singlemode-no core-singlemode fiber coupler (SNSFC) structure. When the light is transmitted from input singlemode fiber (SMF) to the tapered no core fiber (NCF), it will excite multiple cladding modes and coupled to the other NCF which is physically contacted with the input NCF. The light will then be coupled to the two output SMF fibers. The multiple cladding modes in the NCF section will interact with the surrounding environment, thus resulting in a wavelength shift or power variation for the tapered SNSFC structure. Once the wavelength shift or the power variation is calibrated, the change of surrounding environment will be determined.

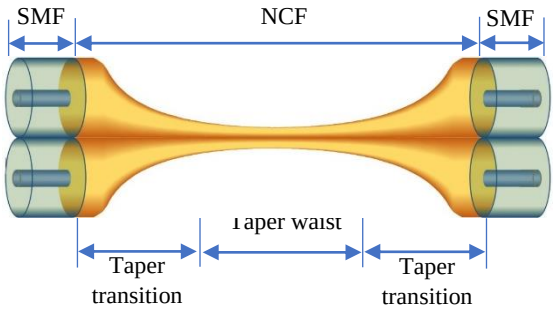


**Fig. 1.** Schematic diagram of SNSFC fiber structure

## 3. Experiments

3.1 The tapered SNSFC structure for refractive index (RI) measurement.

In the experiments, two singlemode-no core-singlemode (SNS) fiber sensor structures were firstly prepared by fusion splicing a short section of NCF (15 mm length) between two SMFs. The NCF used in the experiments is FG125LA purchased from Thorlabs. The fabricated two SNS fiber structures were then aligned and twisted two turns between two fiber holders with a distance of 80 mm, which enables the two SNS fiber structures having good physical contact. The NCF sections of the two SMS fiber structures were then heated to circa 1200 °C that can soften the NCFs, and the two ends of the SNS were pulled by two computer-controlled translation stages for thinning the NCF to form a tapered SNSFC structure. Two tapered SNSFCs with different taper waist diameters

(58.6 and 10.4 µm) were prepared for RI sensitivity measurement. Figure 2(a) shows wavelength shifts of the sensors with two different taper waist diameters at the RI range of 1.33. The sensor with a smaller diameter of 10.4 µm has a higher RI sensitivity of 1523.333 nm/RIU, compared to that of 233.977 nm/RIU for the sensor with a taper waist diameter of 58.6 µm. Therefore, the fiber sensor with a taper diameter of 10.4 µm is selected for further experiments for detection of *S. aureus* (provided from State Key Lab Food Science and Technology, Nanchang University, China). Since *S. aureus* normally survived in phosphate buffered saline (PBS; Catalog number: SH30256.01, pH=7.4, purchased from GE Healthcare Life Sciences) environment, the stability of the biosensor in PBS was firstly tested. Figure 2(b) shows the tapered SNSFC sensors have good stability with maximum wavelength variations of ±0.03 nm over 40 minutes in the PBS.

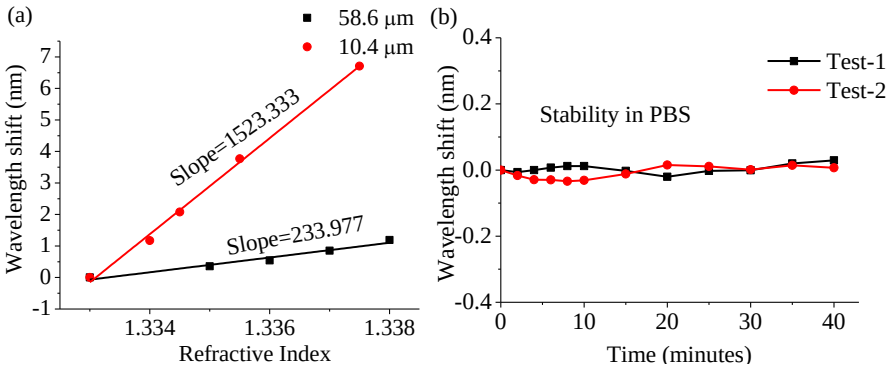


**Fig. 2.** (a) Wavelength shift of the tapered SNSFC vs. RI with two different taper waist diameters (58.6 and 10.4 µm) and (b) stability of the tapered SNSFC sensor in PBS with a taper waist diameter of 10.4 µm.

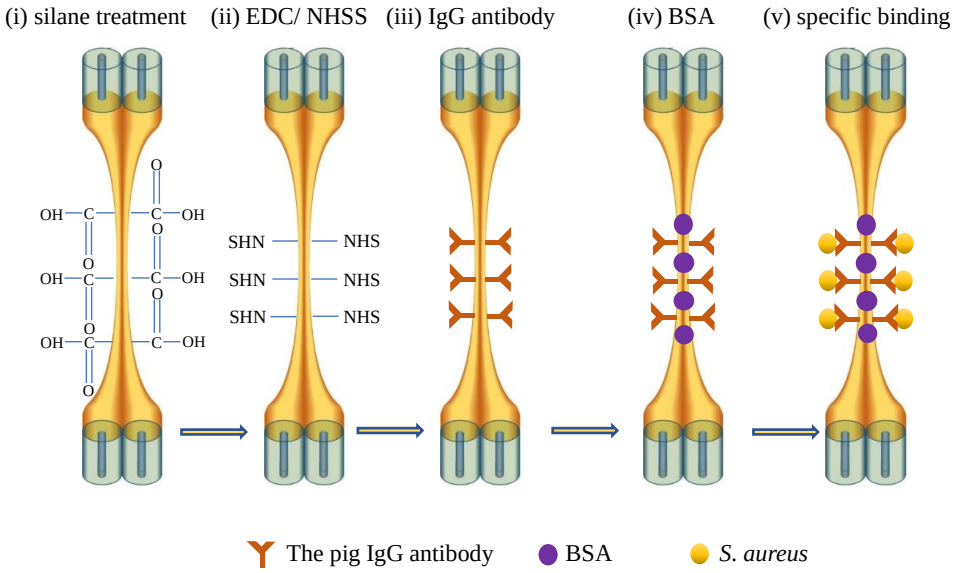


**Fig. 3.** A schematic diagram of fiber surface modification process: (i) treat with silane reagent to create carboxyl group; (ii) generate NHS active ester with EDC/NHSS; (iii) immobilize pig immunoglobulin G (IgG) antibodies on the fiber sensor surface; (iv) block unbind sites with BSA; (v) specific bind with *S. aureus*

### 3.2 Functionalization of the tapered SNSFC sensor

In order to enable the fiber sensor for *S. aureus* detection, the sensor needs to be functionalized with pig IgG antibody (product code: b1108, purchased from BEIJING BERSEE SCIENCE AND TECHNOLOGY CO.LTD, http://www.berseebio.com), which can specifically bind with target *S. aureus* [29-32]. The functionalization process is illustrated below:

i. The fiber sensor is immersed in a solution of 5% silane reagent (3-(3-triethoxysilylpropyl)oxolane-2,5-dione) (product code:T195932-5g, purchased from aladdin) in ethanol for 4 hours at room temperature to create a carboxyl group on the fiber sensor surface.

ii. After cleaning the above fiber with deionized water, the fiber is then immersed into freshly prepared pH buffer(pH=6.0, product code: P118681 and P118682, purchased from aladdin) containing 1-(3-Dimethylaminopropyl)-3-ethylcar-bodiimide hydrochloride (EDC, product code: 39141134, purchased from Sinopharm Chemical Reagent Co., Ltd) for 30 minutes, followed by immediately immersed in a mixed solution of EDC and hydroxy-2,5-dioxopyrolidine-3-sulfonicacid sodium salt (NHSS, product code: H109337, purchased from aladdin) for 30 minutes.

iii. The above fiber sensor is washed with PB buffer and then immersed into a pig IgG antibody solution (in PBS buffer) for 4 hours. This process enables the pig IgG antibody be immobilized on the surface of fiber sensor.

iv. After washing the above fiber with a PBS, the above fiber sensor is then immersed into 1% Bovine serum albumin (BSA, product code: A119741, purchased from aladdin) in PBS for 2 hours at room temperature, then the fiber sensor is cleaned with PBS before being used for detection of *S. aureus*.

A schematic diagram of the fiber sensor surface functionalization process is illustrated in Fig. 3(b): i-iv, which corresponds to above four steps, respectively. The functionalized fiber sensor will specifically bind with *S. aureus* as shown in Fig. 3(b): v.

Figures 4(a) and (b) illustrated scanning electron microscope (SEM) images of the functionalized fiber sensor bind with *S. aureus* (the sphere in Fig. 4).

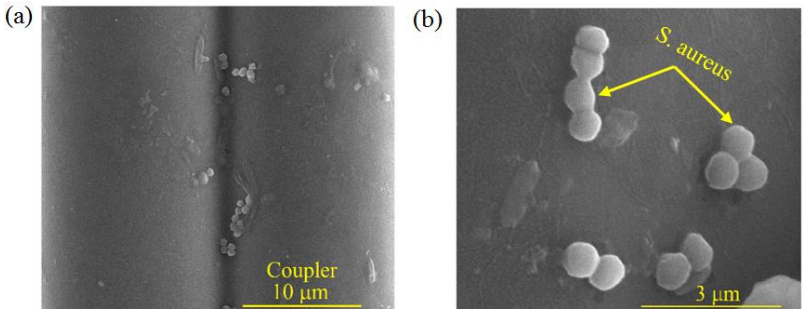


**Fig. 4.** SEM images of (a) the tapered SNSFC bind with *S. aureus*; (b) amplified *S. aureus* bind to the fiber sensor surface.

### 3.3 Detection of *S. aureus*

Figure 5 shows a schematic diagram of the experimental setup for detection of *S. aureus* by using the developed fiber sensor, where a broadband light source (BBS, SC-5-FC) is connected to one of the input SMFs and an optical spectrum analyzer (OSA, YOKOGAWA AQ6370D) is used to measure spectral response of the tapered SNSFC sensor. The fiber coupler sensor section was immersed in a rectangular container (44 *mm*×5 *mm*×5 *mm*), in which different concentrations of *S. aureus* samples were added in sequence (from low to high: $7\times10^1$ CFU/ml, $7\times10^2$ CFU/ml, $7\times10^3$ CFU/ml, $7\times10^4$ CFU/ml) during the tests. Before changing each concentration of *S. aureus* sample, the functionalized sensor was immersed into PBS buffer for 20 minutes to wash out the nonspecific bind *S. aureus*. The fiber sensor was then immersed into *S. aureus* sample for 30 minutes to allow the pig IgG antibodies specifically capture and bind with *S. aureus*, which effectively introduces change of the surrounding RI and coating thickness of the fiber sensor, resulting in change of spectral responses.

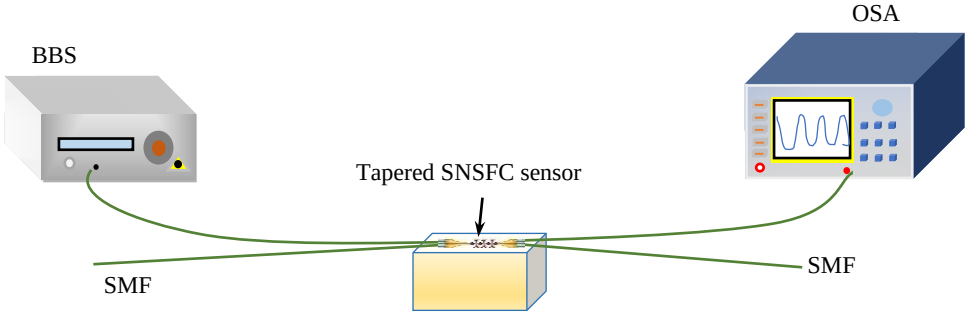


**Fig. 5.** Schematic diagram of the experimental setup of the tapered SNSFC for *S. aureus* detection

## 4. Results and discussion

Investigation of capture layer concentration

The spectral response of the functionalized sensor (sensor surface functionalized with 50 µg/ml pig IgG antibody) at different durations are shown in Fig. 6(a) by immersing the fiber sensor within *S. aureus* solution with a concentration of $7\times10^1$ CFU/ml. The dip wavelength is shifted monotonically to short wavelength side as the time is increased up to 30 minutes.

The influence of the concentration of pig IgG antibody on the performance of the sensor was studied using three different tapered SNSFC structures (fabricated under the same conditions) functionalized with three different concentrations (25 µg/ml, 50 µg/ml and 200 µg/ml) of pig IgG antibody to detect *S. aureus* samples with different concentrations of $7\times10^1$ CFU/ml, $7\times10^2$ CFU/ml, $7\times10^3$ CFU/ml, $7\times10^4$ CFU/ml in sequence, respectively. Figure 6(b) summarized the relationships between time and dip wavelength shifts of the three fiber biosensors immersed in different concentrations of *S. aureus* samples.

It can be clearly seen from Fig. 6(b) that, for all the three fiber biosensors, as the immerse time increases, the dip wavelength shifts monotonically to the short wavelength side, which is due to the binding process of *S. aureus* onto the functionalized fiber sensor surface. It also shows that the higher the *S. aureus* concentration, the larger the dip wavelength shift. Whereas the dip wavelength shift is mainly observed in the initial 20 minutes, after which the spectral responses become stabilized, indicating that the binding process is mainly taken place in the first 20 minutes. During the binding process, the shift of wavelength shows an exponential relationship with immersing time, which is consistent with the kinetic response of the immune behaviour reported in the literature [33]. At the same concentration of *S. aureus*, the sensor functionalized with a higher concentration of pig IgG antibody has a much larger dip wavelength shift and hence a higher sensitivity. The possible reason is that a higher concentration of pig IgG antibody has better capability to capture *S. aureus* and hence result in a larger wavelength shift for the same concentration of *S. aureus*. Reproducibility of the biosensors was investigated by fabricating 15 tapered SNSFC fiber structure with same fabrication parameters. The fabricated 15 tapered SNSFC structures were then functionalized with 25 µg/ml, 50 µg/ml and 200 µg/ml pig IgG antibody, where each concentration of pig IgG antibody is used to modify 5 tapered SNSFC structures. The measurement results were shown in Fig. 6(c), which clearly show that the tapered SNSFC biosensor has a relatively good reproducibility. The average dip wavelength shifts of fiber biosensors modified with 25 µg/ml, 50 µg/ml and 200 µg/ml were 0.25, 0.56, 0.87, 1.20; 0.70, 1.76, 3.09, 4.22 and 2.04 nm, 3.73 nm, 5.25 nm, 7.58 nm for different concentrations ($7\times10^1$ CFU/ml, $7\times10^2$ CFU/ml, $7\times10^3$ CFU/ml, $7\times10^4$ CFU/ml) of *S. aureus.* It is noted that, in the above calculation of average dip wavelength shift, the accumulated wavelength variations in PBS solution as shown in Fig. 6(b) weren't counted. Figure 6(c) also shows that the fiber biosensor has largest error bar at the lowest concentration of $7\times10^1$ CFU/ml compared to that of highest concentration of $7\times10^4$ CFU/ml. This is possibly because that number of *S. aureus* of one colony isn't certain and the higher concentration of *S. aureus* sample will have better average effect compared to that of lower concentration of *S. aureus* sample, and thus smaller measurement difference with different fiber biosensors. When the concentration of *S. aureus* is $7\times10^1$ CFU/ml, the sensor functionalized with pig IgG antibody concentration of 200 µg/ml has the largest average wavelength shift of 2.04 nm. Since the wavelength variation of the fiber sensor in PBS is within ±0.03 nm, the LOD for *S. aureus* reachs 3.1 CFU/ml provided the measurement limit is defined as 3 times of the wavelength variation (0.09 nm).

The specificity of the biosensor was further investigated by immersing three identical sensors (functionalized with 50 µg/ml pig IgG antibody) into three different analytes (varying from large bacteria *E.Coli* to small protein hCG), namely $4\times10^6$ CFU/ml *E. coli*, 10 mg/ml BSA and 50 mIU/ml hCG and each analytes were tested five times. Experimental results combined with measurement of *S. aureus* with concentration of $7\times10^4$ CFU/ml are shown in Fig.6 (e). The average dip wavelength shifts of identical sensors were observed to be 4.22; 0.14; 0.23; and 0.42 nm for the *S. aureus*, *E. coli*, BSA and hCG respectively, indicating that the biosensor has relatively good specificity and reproducibility.

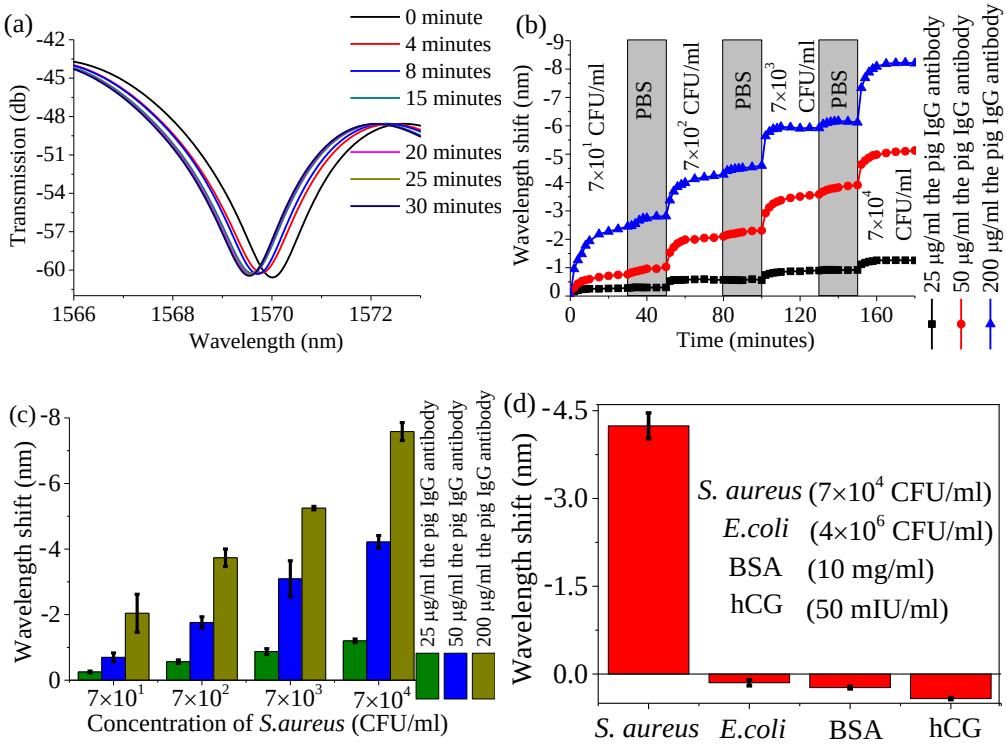


**Fig. 6.** (a) Spectral responses of the tapered SNSFC sensor functionalized with 50 µg/ml pig IgG antibody for detection of *S. aureus* with concentration of $7\times10^1$ CFU/ml; (b) comparison of different capture layer concentrations (25 µg/ml, 50 µg/ml, 200 µg/ml) for *S. aureus* detection; (c) reproducibility and (d) specificity results of the biosensor.

**Table 1** A summary of optical biosensor techniques used for the detection of pathogenic bacteria

| Transducer | Pathogenic bacteria | LOD | Reference |
|---|---|---|---|
| Long-period fiber gratings (LPFGs) | *S. aureus* | 224 CFU/ml | [34] (2019) |
| A fiber optic SPR immunosensor with functionalized molybdenum disulfide (MoS2) nanosheets | *E. coli* | 94 CFU/mL | [35] (2019) |
| Fluorescent (optical) bioprobe | *S. aureus* | 85 CFU/mL | [36] (2019) |
| Multi-column capillary biosensor based on Fenanocluster amplification and smart phone imaging | *Salmonella Typhimurium (S. Typhimurium)* | 14 CFU/mL | [37] (2019) |
| Multimode microfiber | *E. coli* | $10^3$ CFU/ml | [38] (2018) |
| Single mode-tapered multimode-single mode (SMS) | *S. Typhimurium* | 247 CFU/mL | [39] (2018) |
| Microfluidic biosensor based on fluorescence labelling and smartphone video processing | *S. Typhimurium* | 58 CFU/mL | [40] (2019) |
| Fluorescence imaging biosensor by smartphone | *S. aureus* | 10 CFU/mL | [41] (2018) |
| Microcavity in-line Mach-Zehnder | *Live E. coli* | 100 CFU/mL | [42] (2018) |

| | | | |
|---|---|---|---|
| interferometer | | | |
| Tapered SNSFC biosensor | *S. aureus* | **3.1 CFU/mL** | **Proposed method in this paper** |

The performance comparison between our newly developed fiber biosensor and those of recently published optical biosensor techniques for the detection of bacteria are shown in Table 1. The LOD of our proposed sensor is as low as 3.1 CFU/ml, which is the best result reported so far by using optical fiber sensors, demonstrating the significant advantage of our proposed sensor.

As for the lifetime of the sensor, our initial tests showed that after storage 3 days at room temperature or 6 days in a fridge at 3-5 ℃, the optical fiber biosensors functionalized with the pig IgG antibody still worked very well. When the storage time was longer than the indicated days, the activity of the fiber biosensor functionalized with pig IgG antibody decreased significantly.

## 5. Conclusion

In conclusion, an ultra-highly sensitive tapered SNSFC label-free biosensor for measurement of *S. aureus* is proposed and experimentally demonstrated. The tapered SNSFC sensor is composed of two parallel physical contact SNS fiber structures, where the two NCF sections are heated to be tapered to small diameter. The tapered SNSFC fiber sensor is then functionalized with pig IgG antibody which can specifically bind with *S. aureus*. Experimentally, for the tapered SNSFC sensor with a taper waist diameter of 10.4 μm and functionalized with 200 μg/ml pig IgG antibody, an average wavelength shift of 2.04 nm is obtained over a period of 30 minutes for the measurement of *S. aureus* with concentration of $7\times10^1$ CFU/ml. The tapered SNSFC has a large taper waist dimension (two 10.4 μm diameter fibers), and hence has a good stability, which has been demonstrated by achieving a maximum wavelength variation of ±0.03 nm in the PBS for 40 minutes. The LOD of the biosensor is calculated as low as 3.1 CFU/ml, showing an ultrahigh sensitivity. The developed tapered SNSFC sensor structure can be used for various applications such as earlier diseases/medical diagnostics and food safety inspection once the fiber sensor is properly functionalized.


## Acknowledgements

This work was supported by the Nanchang Hangkong University graduate student innovation special fund project (Grant No. YC2019049), Natural Science Foundation of Jiangxi Province (Grant No. 20192ACB20031 and 20192ACBL21051); State Key Laboratory of Advanced Optical Communication Systems and Networks, Shanghai Jiao Tong University, China (Grant No. 2018G2KF03003); the National Natural Science Foundation of China (Grant No. 61665007 and 61465009); Major academic and technical leaders funding program of Jiangxi, China (Grant No. 20172BCB22012).


## References


[1] A. Ogston, "On Abscesses," Clin. Infect. Dis. 6 (1984) 122-128. https://doi.org/10.1093/clinids/6.1.122.

[2] R.H. Deurenberg, E.E. Stobberingh, The evolution of *Staphylococcus aureus*, Infect. Genet. Evol. 8 (2008) 747-763. https://doi.org/10.1016/j.meegid.2008.07.007.

[3] J.A. Hennekinne, M.L. De Buyser, S. Dragacci, *Staphylococcus aureus* and its food poisoning toxins: Characterization and outbreak investigation, FEMS Microbiol. Rev. 36 (2012) 815-836. https://doi.org/10.1111/j.1574-6976.2011.00311.x.

[4] M. Otto, *Staphylococcus aureus* toxins, Curr. Opin. Microbiol. 17 (2014) 32-37. https://doi.org/10.1016/j.mib.2013.11.004.

[5] A. Pantosti, A. Sanchini, M. Monaco, Mechanisms of antibiotic resistance in *Staphylococcus aureus*. Future Microbiol. 2 (2007) 323-334. https://doi.org/10.2217/17460913.2.3.323.

[6] B. Alarcón, B. Vicedo, R. Aznar, PCR-based procedures for detection and quantification of *Staphylococcus aureus* and their application in food, J. Appl. Microbiol. 100 (2006) 352-364. https://doi.org/10.1111/j.1365-2672.2005.02768.x.

[7] T. Trnčíková, V. Hrušková, K. Oravcová, D. Pangallo, E. Kaclíková, Rapid and sensitive detection of *Staphylococcus aureus* in food using selective enrichment and real-time PCR targeting a new gene marker, Food Anal. Methods. 2 (2009) 241-250. https://doi.org/10.1007/s12161-008-9056-x.

[8] R.W. Bennett, Staphylococcal enterotoxin and its rapid identification in foods by enzyme-linked immunosorbent assay-based methodology, J. Food Prot. 68 (2005) 1264-1270. https://doi.org/10.4315/0362-028X-68.6.1264.

[9] K.C. Carroll, Rapid diagnostics for methicillin-resistant *Staphylococcus aureus*: Current status, Mol. Diagnosis Ther. 12 (2008) 15-24. https://doi.org/10.1007/BF03256265.

[10] T. Majumdar, R. Chakraborty, U. Raychaudhuri, Development of PEI-GA modified antibody based sensor for the detection of *S. aureus* in food samples, Food Biosci. 4 (2013) 38-45. https://doi.org/10.1016/j.fbio.2013.08.002.

[11] C. Menti, M. Beltrami, M.D. Pozza, S.T. Martins, J.A.P. Henriques, A.D. Santos, F.P. Missell, M. Roesch-Ely, Influence of antibody immobilization strategies on the analytical performance of a magneto-elastic immunosensor for *Staphylococcus aureus* detection, Mater. Sci. Eng. C. 76 (2017) 1232-1239. https://doi.org/10.1016/j.msec.2017.03.107.

[12] M. Rubab, H.M. Shahbaz, A.N. Olaimat, D.H. Oh, Biosensors for rapid and sensitive detection of *Staphylococcus aureus* in food, Biosens. Bioelectron. 105 (2018) 49-57. https://doi.org/10.1016/j.bios.2018.01.023.

[13] Q. Wu, Y. Semenova, P. Wang, G. Farrell, High sensitivity SMS fiber structure based refractometer - analysis and experiment, Opt. Express. 19 (2011) 7937-7944. https://doi.org/10.1364/oe.19.007937.

[14] L.L. Liu, L. Marques, R. Correia, S.P. Morgan, S.W. Lee, P. Tighe, L. Fairclough, S. Korposh, Highly sensitive label-free antibody detection using a long period fibre grating sensor, Sensors Actuators, B Chem. 271 (2018) 24-32.

[15] R. Srinivasan, S. Umesh, S. Murali, S. Asokan, S. Siva Gorthi, Bare fiber Bragg grating immunosensor for real-time detection of *Escherichia coli* bacteria, J. Biophotonics. 10 (2017) 224–230. https://doi.org/10.1002/jbio.201500208.

[16] M.A. Cooper, Label-free screening of bio-molecular interactions, Anal. Bioanal. Chem. 377 (2003) 834-842. https://doi.org/10.1007/s00216-003-2111-y.

[17] M.A. Mustapa, M.H. Abu Bakar, Y. Mustapha Kamil, A. Syahir, M.A. Mahdi, Bio-Functionalized Tapered Multimode Fiber Coated with Dengue Virus NS1 Glycoprotein for Label Free Detection of Anti-Dengue Virus NS1 IgG Antibody, IEEE Sens. J. 18 (2018) 4066-4072. https://doi.org/10.1109/JSEN.2018.2813385.

[18] A. Leung, K. Rijal, P.M. Shankar, R. Mutharasan, Effects of geometry on transmission and sensing potential of tapered fiber sensors, Biosens. Bioelectron. 21 (2006) 2202–2209. https://doi.org/10.1016/j.bios.2005.11.022.

[19] H. Zhang, X. Ma, Y. Liu, N. Duan, S. Wu, Z. Wang, B. Xu, Gold nanoparticles enhanced SERS aptasensor for the simultaneous detection of *Salmonella typhimurium* and *Staphylococcus aureus*, Biosens. Bioelectron. 74 (2015) 872-877.

[20] Y.J. Sung, H.J. Suk, H.Y. Sung, T. Li, H. Poo, M.G. Kim, Novel antibody/gold nanoparticle/magnetic nanoparticle nanocomposites for immunomagnetic separation and rapid colorimetric detection of *Staphylococcus aureus* in milk, Biosens. Bioelectron. 43 (2013) 432-439. https://doi.org/10.1016/j.bios.2012.12.052.

[21] X. He, Y. Li, D. He, Aptamer-fluorescent silica nanoparticles bioconjugates based dual-color flow cytometry for specific detection of *S. aureus*. J. Biomed. Nanotechnol. 10 (2014) 1359-1368. https://doi.org/10.1166/jbn.2014.1828.

[22] R. Bharadwaj, V.V.R. Sai, K. Thakare, A. Dhawangale, T. Kundu, S. Titus, P.K. Verma, S. Mukherji, Evanescent wave absorbance based fiber optic biosensor for label-free detection of *E. coli* at 280nm wavelength, Biosens. Bioelectron. 26 (2011) 3367-3370. https://doi.org/10.1016/j.bios.2010.12.014.

[23] Y. Yang, K. Xiong, Y. Tan, B. Liu, Y. Sun, D. Chen, H. Tan, Direct monitoring of antigen-antibody interactions by optical fiber bioprobe, Third Int. Conf. Photonics Imaging Biol. Med. 5254 (2003) 431-436. https://doi.org/10.1117/12.546220.

[24] S.M. Tripathi, W.J. Bock, P. Mikulic, R. Chinnappan, A. Ng, M. Tolba, M. Zourob, Long period grating based biosensor for the detection of *Escherichia coli* bacteria, Biosens. Bioelectron. 35 (2012) 308-312. https://doi.org/10.1016/j.bios.2012.03.006.

[25] T. Liu, Y. Zhao, Z. Zhang, P. Zhang, J. Li, R. Yang, C. Yang, L. Zhou, A fiber optic biosensor for specific identification of dead *Escherichia coli O157:H7*, Sensors Actuators, B Chem. 196 (2014) 161-167. https://doi.org/10.1016/j.snb.2014.02.003.

[26] M. Janczuk-Richter, M. Dominik, E. Roźniecka, M. Koba, P. Mikulic, W.J. Bock, M. Łoś, M. Śmietana, J. Niedziółka‐Jönsson, Long-period fiber grating sensor for detection of viruses, Sensors Actuators, B Chem. 250 (2017) 32-38. https://doi.org/10.1016/j.snb.2017.04.148.

[27] H.N. Abdelhamid, H.F. Wu, Selective biosensing of *Staphylococcus aureus* using chitosan quantum dots, Spectrochim. Acta - Part A Mol. Biomol. Spectrosc. 188 (2018) 50-56. https://doi.org/10.1016/j.saa.2017.06.047.

[28] R. Kumar, Y. Leng, B. Liu, J. Zhou, L. Shao, J. Yuan, X. Fan, S. Wan, T. Wu, J. Liu, R. Binns, Y.Q. Fu, W.P. Ng, G. Farrell, Y. Semenova, H. Xu, Y. Xiong, X. He, Q. Wu, Ultrasensitive biosensor based on magnetic microspheres enhanced microfiber interferometer, Biosens. Bioelectron. 145 (2019) 111563. https://doi.org/10.1016/j.bios.2019.111563.

[29] J. Deisenhofer Crystallographic Refinement and Atomic Models of a Human Fc Fragment and Its Complex with Fragment B of Protein A from *Staphylococcus aureus* at 2.9- and 2.8-Å Resolution, Biochemistry. 20 (1981) 2361-2370. https://doi.org/10.1021/bi00512a001.

[30] W. Kong, J. Xiong, H. Yue, Z. Fu, Sandwich Fluorimetric Method for Specific Detection of *Staphylococcus aureus* Based on Antibiotic-Affinity Strategy, Anal. Chem. 87 (2015) 9864-9868. https://doi.org/10.1021/acs.analchem.5b02301.

[31] H. Gao, S. Yang, J. Han, J. Xiong, W. Kong, C. Li, G. Liao, Z. Fu, Double-site recognition of pathogenic bacterial whole cells based on an antibiotic-affinity strategy, (2015) 12497-12500. https://doi.org/10.1039/c5cc02814k.

[32] X. Meng, G. Yang, F. Li, T. Liang, W. Lai, H. Xu, Sensitive Detection of *Staphylococcus aureus* with Vancomycin-Conjugated Magnetic Beads as Enrichment Carriers Combined with Flow Cytometry, ACS Appl. Mater. Interfaces. 9 (2017) 21464-21472. https://doi.org/10.1021/acsami.7b05479.

[33] G. Liu, K. Li, Micro/nano optical fibers for label-free detection of abrin with high sensitivity, Sensors Actuators, B Chem. 215 (2015) 146–151. https://doi.org/10.1016/j.snb.2015.03.056.

[34] F. Yang, T.L. Chang, T. Liu, D. Wu, H. Du, J. Liang, F. Tian, Label-free detection of *Staphylococcus aureus* bacteria using long-period fiber gratings with functional polyelectrolyte coatings, Biosens. Bioelectron. 133 (2019) 147-153. https://doi.org/10.1016/j.bios.2019.03.024.

[35] S. Kaushik, U.K. Tiwari, S.S. Pal, R.K. Sinha, Rapid detection of *Escherichia coli* using fiber optic surface plasmon resonance immunosensor based on biofunctionalized Molybdenum disulfide (MoS 2 ) nanosheets, Biosens. Bioelectron. 126 (2019) 501-509. https://doi.org/10.1016/j.bios.2018.11.006.

[36] N. Bhardwaj, S.K. Bhardwaj, D. Bhatt, S.K. Tuteja, K.H. Kim, A. Deep, Highly sensitive optical biosensing of: *Staphylococcus aureus* with an antibody/metal-organic framework bioconjugate, Anal. Methods. 11 (2019) 917-923. https://doi.org/10.1039/c8ay02476f.

[37] H. Zhang, L. Xue, F. Huang, S. Wang, L. Wang, N. Liu, J. Lin, A capillary biosensor for rapid detection of *Salmonella* using Fe-nanocluster amplification and smart phone imaging, Biosens. Bioelectron. 127 (2019) 142-149. https://doi.org/10.1016/j.bios.2018.11.042.

[38] Y. Li, H. Ma, L. Gan, A. Gong, H. Zhang, D. Liu, Q. Sun, Selective and sensitive *Escherichia coli* detection based on a T4 bacteriophage-immobilized multimode microfiber, J. Biophotonics. 11 (2018) 1-8. https://doi.org/10.1002/jbio.201800012.

[39] S. Kaushik, A. Pandey, U.K. Tiwari, R.K. Sinha, A label-free fiber optic biosensor for *Salmonella Typhimurium* detection, Opt. Fiber Technol. 46 (2018) 95-103. https://doi.org/10.1016/j.yofte.2018.09.012.

[40] S. Wang, L. Zheng, G. Cai, N. Liu, M. Liao, Y. Li, X. Zhang, J. Lin, A microfluidic biosensor for online and sensitive detection of *Salmonella typhimurium* using fluorescence labeling and smartphone video processing, Biosens. Bioelectron. 140 (2019) 111333. https://doi.org/10.1016/j.bios.2019.111333.

[41] S. Shrivastava, W. Il Lee, N.E. Lee, Culture-free, highly sensitive, quantitative detection of bacteria from minimally processed samples using fluorescence imaging by smartphone, Biosens. Bioelectron. 109 (2018) 90-97. https://doi.org/10.1016/j.bios.2018.03.006.

[42] M. Janik, M. Koba, A. Celebańska, W.J. Bock, M. Śmietana, Live *E. coli* bacteria label-free sensing using a microcavity in-line Mach-Zehnder interferometer, Sci. Rep. 8 (2018) 4-11. https://doi.org/10.1038/s41598-018-35647-2.